THE JOURNAL OF BIOLOGICAL CHEMISTRY Vol. 279, No. 11, Issue of March 12, pp. 10624–10633, 2004
Printed in U.S.A.

Role of the Histidine Triad-like Motif in Nucleotide Hydrolysis by the Rotavirus RNA-packaging Protein NSP2*

Received for publication, October 22, 2003, and in revised form, December 16, 2003
Published, JBC Papers in Press, December 29, 2003, DOI 10.1074/jbc.M311563200

Rodrigo Vasquez-Del Carpio‡§¶, Fernando D. González-Nilo‖, Hariharan Jayaram‡‡, Eugenio Spencer§, B. V. Venkataram Prasad**‡‡, John T. Patton‡, and Zenobia F. Taraporewala‡§§**

*From the ‡Laboratory of Infectious Diseases, NIAID, National Institutes of Health, Bethesda, Maryland 20892, the §Laboratorio de Virologia and the ‖Departamento de Ciencias Químicas, Facultad de Química y Biología, Universidad de Santiago de Chile, Casilla 40 Correo 33, Santiago, Chile, and the **Verna and Marrs McLean Department of Biochemistry and Molecular Biology, Baylor College of Medicine, Houston, Texas 77030*

Octamers formed by the nonstructural protein NSP2 of rotavirus are proposed to function as molecular motors in the packaging of the segmented double-stranded RNA genome. The octamers have RNA binding, helix unwinding, and Mg^{2+}-dependent NTPase activities and play a crucial role in assembly of viral replication factories (viroplasms). Comparison of x-ray structures has revealed significant structural homology between NSP2 and the histidine triad (HIT) family of nucleotidyl hydrolases, which in turn has suggested the location of the active site for NTP hydrolysis in NSP2. Consistent with the structural predictions, we show here using site-specific mutagenesis and ATP docking simulations that the active site for NTP hydrolysis is localized to residues within a 25-Å-deep cleft between the C- and N-terminal domains of the NSP2 monomer. Although lacking the precise signature HIT motif (HØHØHØØ where Ø is a hydrophobic residue), our analyses demonstrate that histidines (His^{221} and His^{225}) represent critical residues of the active site. Similar to events occurring during nucleotide hydrolysis by HIT proteins, NTP hydrolysis by NSP2 was found to produce a short lived phosphorylated intermediate. Evaluation of the biological importance of the NTPase activity of NSP2 by transient expression in mammalian cells showed that such activity has no impact on the ability of NSP2 to induce the hyperphosphorylation of NSP5 or to interact with NSP5 to form viroplasm-like structures. Hence the NTPase activity of NSP2 probably has a role subsequent to the formation of viroplasms, consistent with its suspected involvement in RNA packaging and/or replication.

Rotaviruses, members of the Reoviridae, are a major cause of acute gastroenteritis in infants and young children worldwide (1). The virion is a triple layered icosahedron with a genome consisting of 11 segments of double-stranded RNA that encode for six structural and six nonstructural proteins (2). NSP2 is a conserved, basic nonstructural protein (M_r = 35,000) encoded by the virus that is necessary for replication and packaging (3, 4). NSP2 self-assembles into stable octamers that possess Mg^{2+}-dependent NTPase activity (5, 6). This activity is associated with autophosphorylation of the protein via linkage of the cleaved γ-phosphate (6). The NSP2 octamers also have strong, sequence-independent single-stranded RNA binding activity capable of destabilizing RNA-RNA duplexes by an ATP- and Mg^{2+}-independent process (7). The activities of NSP2 when considered in concert with the ability of the octamers to undergo nucleotide-induced conformational shifts favor a role for NSP2 during replication as a molecular motor (8). It can be predicted that NSP2 unwinds the template single-stranded RNA and functions, in coordination with the viral RNA polymerase, to overcome the entropy of genome packaging prior to or as the single-stranded RNA is replicated to double-stranded RNA.

NSP2 co-localizes with NSP5, an *O*-linked glycosylated phosphoprotein, to cytoplasmic inclusions (viroplasms) that form in infected cells (9–11). Viroplasms are viral factories in which genome packaging, replication, and early steps in virion morphogenesis are presumed to occur (10, 12). When expressed in combination, NSP2 and NSP5 co-localize and form viroplasm-like structures in uninfected cells (13). NSP5 has weak autokinase activity and *in vivo* is found in several phosphorylated isoforms (28 and 32–34 kDa) (14). The function of NSP5 phosphorylation is not known but has been correlated with its localization to viroplasms and its association with NSP2 (15, 16). NSP5, like NSP2, is a nonspecific RNA-binding protein and a component of replication intermediates (17–20).

The structure of the NSP2 octamer, recently solved at 2.6 Å, has led to suggestions concerning the nature of its interactions with NTP and RNA. NSP2 crystallized as a 4-2-2 octamer made up of two tetramers stacked tail-to-tail (Ref. 21 and Fig. 1). Along the outer surface of the octamer are four highly basic grooves that probably serve as RNA-binding sites. NTP was proposed to bind to NSP2 within a 25-Å-deep cleft that forms between the C- and N-terminal domains of the monomer (Ref. 21 and Fig. 1.). The location of the NTP-binding site was based on the superposition of the C-terminal domain of NSP2 with the catalytic core of protein kinase C-interacting protein (PKCI),[1] a prototypical member of the histidine triad (HIT) family of nucleotide-interacting proteins (22). Despite the absence of a precise signature HIT motif (HØHØHØØ where Ø is a hydrophobic residue) in NSP2, significant structural homol-

* This work was supported in part by a grant from the Fondo Nacional de Desarrollo Científico y Tecnológico, Chile (to E. S.). The costs of publication of this article were defrayed in part by the payment of page charges. This article must therefore be hereby marked "*advertisement*" in accordance with 18 U.S.C. Section 1734 solely to indicate this fact.

¶ Supported by fellowships from the German Academic Exchange Service (Deutscher Akademischer Austausch Dienst) and from the Comisión Nacional de Investigación Científica y Tecnológica, Chile.

‡‡ Supported by NIH Grant AI36040.

§§ To whom correspondence should be addressed: Laboratory of Infectious Diseases, NIAID, National Institutes of Health, 50 South Dr., MSC 8026, Rm. 6314, Bethesda, MD 20892. Tel.: 301-594-1663; Fax: 301-496-8312; E-mail: ztarapore@niaid.nih.gov.

[1] The abbreviations used are: PKCI, protein kinase C-interacting protein; HIT, histidine triad; wt, wild-type; mt, mutant; BSA, bovine serum albumin; CKII, casein kinase II; p.i., postinfection; PBS, phosphate-buffered saline.

ogy with PKCI suggested the existence of a HIT-like motif within its cleft with His^{225} representing the putative catalytic residue for hydrolysis (21).

In this study, we used mutagenesis and computer modeling to identify residues within the cleft that participate in NTP hydrolysis by NSP2. These analyses indicate that His^{225} and other nearby residues of the predicted HIT-like motif of NSP2 are essential for NTPase activity, including two residues predicted to coordinate binding of Mg^{2+}. Using mutant forms of NSP2, we also found that the NTPase activity is required for NSP2 autophosphorylation and NSP5 phosphorylation *in vitro* but that the level of the hydrolysis activity is not a direct predictor of the extent of phosphorylation of either of these proteins. Conversely transient expression studies indicate that the NTPase activity of NSP2, and thus NSP2 or NSP5 phosphorylation, have no role in the formation of viroplasms.

EXPERIMENTAL PROCEDURES

Cell Culture and Viruses—Fetal rhesus monkey kidney cells (MA104) were maintained in Medium 199 supplemented with 5% fetal bovine serum. Simian rotavirus SA11 was propagated and titered in MA104 cells.

Expression Vectors—The bacterial expression vectors pQE60g8 (6) and pQE30g11 (17) encode NSP2 with a C-terminal tag and NSP5 with an N-terminal tag, respectively, of six histidine residues. The NSP2 open reading frame of the pQE60g8 was mutated by PCR using *Pfu* Turbo DNA polymerase (Invitrogen). The following primer pairs were included in amplification reactions to produce pQE60g8 vectors encoding NSP2 with the mutations H110A (5′-TTAGAAAATTTGGTGATACGTAAAG-3′, 5′-A**GC**CCTTATTGATACTACTCGTGATA-3′; pQE60g8/H110A), E153A (5′-GGAGAAATTGTATTTCAAAACGC-3′, 5′-TCCT**G**CTGCAGTTATTGTAGTTTCAA-3′; pQE60g8/E153A), Y171A (5′-**GC**TTTAGAACATCAATTGATGCCAA-3′; 5′-AGTTAGTTTCCACATGGTGAAGGC-3′; pQEg8/Y171A), K188A (5′-**GC**AGTTACATTGAACGAAGATAAACC-3′, 5′-ATATTCAATAAAATTCTGATCCAG-3′; pQE60g8/K188A), H221A (5′-ACA**GC**TGGTAAGGGTCATTATAGAATTG-3′, 5′-GATTACAGCAAACTTGTTATATTGCC-3′ pQE60g8/H221A), K223A (5′-ACACATGGT**GC**GGGTCATTATAGAATTG-3′, 5′-GATTACAGCAAACTTGTTATATTGCC-3′; pQE60g8/K223A), H225A (5′-ACACATGGTAAGGGT**GC**TTATAGAATTG-3′, 5′-GATTACAGCAAACTTGTTATATTGCC-3′; pQE60g8/H225A), and R227A (5′-ACACATGGTAAGGGTCATTAT**GC**AATTG-3′, 5′-GATTACAGCAAACTTGTTATATTGCC-3′; pQE60g8/R227A) (bases in primers used to change codons in the open reading frame for NSP2 to those for alanine are shown in bold). Following amplification (94 °C for 2 min, 1 cycle; 94 °C for 30 s, 50 °C for 30 s, 68 °C for 4 min, 35 cycles; 68 °C for 6 min, 1 cycle), products were gel-purified, treated with T4 DNA kinase, self-ligated, and transformed into *Escherichia coli* DH5α. Appropriate plasmids were identified by DNA sequencing and transformed into *E. coli* M15(pREP4).

The T7 transcription vectors SP72g8, SP72g8/E153A, SP72g8/K188A, and SP72g8/H225A, which contain complete open reading frames for either wild-type (wt) or mutant (mt) NSP2, were generated by PCR amplification of the coding region of pQE60g8, pQE60g8/E153A, pQE60g8/K188A, and pQE60g8/H225A, respectively. Amplification reaction mixtures also contained Elongase DNA polymerase (Invitrogen) and the primer pair 5′-CGGAATTCATGGCTGAGCTAGCTTGC-3′ (EcoRI site underlined) and 5′-CCGCTCGAGTTAAACGCCAACTTGAGA-3′ (XhoI site underlined). The amplification conditions were as follows: 94 °C for 3 min, 1 cycle; 94 °C for 1 min, 45 °C for 1 min, 68 °C for 2.5 min, 40 cycles. The amplified DNA product was digested with EcoRI and XhoI and ligated into SP72. To construct the T7 transcription vector pGEM-4Z/g11, a fragment containing the open reading frame for SA11 NSP5 was released from pBR322g11 (23) (a gift of Gerry Both) by digestion with HinPI and SacI and ligated into the AccI and SacI sites of pGEM-4Z. All plasmid contructs with the appropriate inserts were identified by DNA sequencing.

Preparation of NSP2 and NSP5—NSP2 and NSP5 were expressed in *E. coli* M15(pREP4) using the vectors pQE60g8 and pQE30g11, respectively, and purified from bacteria lysates by nickel-nitrilotriacetic acid affinity chromatography (6, 17). NSP2 was dialyzed against low salt buffer (LSB) (2 mM Tris-HCl (pH 7.2), 0.5 mM EDTA, 0.5 mM dithiothreitol). NSP5 was dialyzed briefly against 50 mM NaH_2PO_4 (pH 8.0) and 300 mM NaCl and then dialyzed extensively against LSB with 75 mM NaCl and 0.1% Triton X-100. Protein concentrations were determined by Bradford assay using bovine serum albumin (BSA) as the standard and by co-electrophoresis with known amounts of BSA by 12% SDS-PAGE followed by staining with Coomassie Blue. Recombinant NSP2 was purified to near homogeneity using conditions described previously to obtain protein for crystallization (6). Recombinant NSP5 contained trace (<1%) levels of DnaK (17).

NTPase Assay—Reaction mixtures contained wt or mt NSP2 in 50 mM Tris-HCl (pH 7.5), 5 mM $MgCl_2$, and 10 μCi of [α-^{32}P]ATP (3,000 Ci/mmol) in a final volume of 20 μl. After incubation for 1 h at 37 °C, ADP and ATP in the mixtures were resolved by ascending TLC (6). Radiolabeled spots on the sheets were detected by autoradiography and quantified with a PhosphorImager. ADP and AMP markers were generated from [α-^{32}P]ATP using tobacco acid pyrophosphatase. Percentage of ATP hydrolysis = {quantity of [α-^{32}P]ADP/(quantities of [α-^{32}P]ADP + [α-^{32}P]ATP)} $\times$ 100. The ATP hydrolysis value was corrected for background by subtracting the value obtained for a reaction mixture containing no protein. Relative specific NTPase activity represents the average ATP hydrolysis value/μg of protein as calculated from five assays carried out in parallel with each containing a different concentration of protein.

In Vitro Phosphorylation of NSP2 and NSP5—Reaction mixtures for NSP2 autophosphorylation contained 28 pmol of NSP2, 50 mM Tris-HCl (pH 7.5), 5 mM $MgCl_2$, and 10 μCi of [γ-^{32}P]ATP (3,000 Ci/mmol) in a final volume of 20 μl and were incubated for 1 h at 37 °C. Reaction mixtures for NSP5 phosphorylation contained 70 pmol of NSP5, 28 pmol of NSP2, or no NSP2 and otherwise contained the same components as used in NSP2 autophosphorylation assays. NSP5 phosphorylation assays were incubated for 2 h at 37 °C. Phosphorylated NSP2 and NSP5 were detected by SDS-PAGE and autoradiography and quantified with a PhosphorImager.

Hydrolytic Stability of NSP2 under Acid/Alkaline Conditions—Reaction mixtures for NSP2 autophosphorylation contained 28 pmol of NSP2, 50 mM Tris-HCl (pH 7.5), 5 mM $MgCl_2$, and 10 μCi of [γ-^{32}P]ATP (3,000 Ci/mmol) in a final volume of 20 μl and were incubated for 1 h at 37 °C. The control reaction mixture contained 500 units of casein kinase II (New England BioLabs), casein kinase II (CKII) buffer (20 mM Tris, pH 7.5, 50 mM KCl, 10 mM $MgCl_2$) and 10 μCi of [γ-^{32}P]ATP in a final volume of 20 μl and was incubated for 30 min at 30 °C. Phosphorylated proteins were separated by 12% SDS-PAGE and transferred to polyvinylidene difluoride membrane (Invitrogen). Membranes were air-dried and autoradiographed directly or after an individual incubation at 65 °C for 2 h in alkaline (1 M KOH) or acid (6 M HCl) conditions.

Transient Expression of NSP2 and NSP5 in Vivo—Nearly confluent monolayers of MA104 cells were infected at a multiplicity of infection of ~10 with SA11 rotavirus. At 1 h postinfection (p.i.), the inoculum was replaced with Medium 199, and the cells were further incubated for 8 h before being processed for immunofluorescence microscopy. To transiently express NSP2 and NSP5 *in vivo*, MA104 cells were infected with recombinant vaccinia virus vTF7.3 (24) at a multiplicity of infection of 10. At 1 h p.i., the inoculum was removed and replaced with a transfection mixture consisting of 4% LipofectAMINE (Invitrogen) and 1 μg of one or more T7 transcription vectors expressing NSP2 and/or NSP5. The cells were processed for immunofluorescence at 16 h p.i.

Immunofluorescence Analysis—MA104 cells infected with rotavirus or transiently expressing NSP2 and/or NSP5 were washed with phosphate-buffered saline (PBS), fixed with 4% formaldehyde in PBS for 1 h at room temperature, and again washed with PBS. The cells were initially incubated in PBS containing 5% γ-globulin-free BSA for 15 min at room temperature and then washed with PBS containing 1% Triton X-100. Afterward the cells were incubated with NSP2-specific guinea pig polyclonal antibody (6) and/or NSP5-specific mouse monoclonal antibody 158G37 (15) at a dilution of 1:1,000 in PBS containing 3% BSA for 1.5 h. The cells were then washed successively with PBS containing 1% Triton X-100, PBS containing 1% Triton X-100 and 3% BSA, and PBS containing 1% Triton X-100. Secondary antibodies conjugated to fluorescent dyes, Alexa Fluor 488 goat anti-guinea pig IgG and/or Alexa Fluor 594 goat anti-mouse IgG (Molecular Probes), at a dilution of 1:1,000 in PBS containing 3% BSA were incubated with the cells for 1.5 h. The cells were washed with PBS containing 1% Triton X-100 and with PBS alone and then incubated in PBS containing 3% BSA and 0.1 M glycine for 10 min and in the same buffer containing 6 μg of Hoechst 33258 (4,6-diamidino-2-phenylindole, Pierce)/ml for 10 min to stain nuclei. Following successive washes with PBS containing 1% Triton X-100 and PBS alone, the coverslips were mounted in ProLong Antifade (Molecular Probes). Fluorescence was detected on a Leica TCS NT inverted confocal microscope with an attached UV laser (Coherent, Santa Clara, CA). Images were overlaid using Adobe PhotoShop Version 5.5.

Radiolabeling of NSP2 and NSP5 in Vivo—MA104 cells were in-

fected at a multiplicity of infection of ~10 with SA11 rotavirus. At 1 h p.i., the inoculum was replaced with Medium 199. At 8 h p.i., the medium was replaced with either Cys-,Met-free minimal essential medium or phosphate-free minimal essential medium. At 9 h p.i., these media were replaced respectively with Cys-,Met-free minimal essential medium containing 25 μCi of [^{35}S]methionine/ml (>1,000 Ci/ml, PerkinElmer Life Sciences) and with phosphate-free Dulbecco's minimal essential medium containing 25 μCi of [^{32}P]orthophosphate/ml (9,000 Ci/mmol). After incubation for 3 h, the cells were lysed in 20 mM Tris-HCl (pH 8.0), 137 mM NaCl, 10% glycerol, 1% Nonidet P-40, and 2 μg of aprotinin and 0.5 μg of leupeptin/ml. The lysate was clarified by centrifugation at 10,000 $\times$ *g* for 2 min. For vTF7.3-infected cells programmed to transiently express NSP2 and/or NSP5, the cells were labeled beginning at 14 h p.i. with [^{35}S]methionine or [^{32}P]orthophosphate and harvested as described above.

Molecular Simulation—The crystallographic data of rotavirus NSP2 (Protein Data Bank code 1L9V) was used for all calculations. The hydrogen atoms of the protein were assigned using CHARMm (Version 27) (25) and then energy-minimized using a simulated annealing protocol. The simulated annealing consisted of 500 ps with an initial and a final temperature of 450 and 200 K, respectively. The temperature was decreased in steps of 5 K/10 ps. The other non-hydrogen atoms were restrained during this simulation. The calculations were performed using a distance-dependent dielectric constant of 80. The Autodock 3.02 (26) program was then used with the energy minimized NSP2 structure to perform a docking simulation of an ATP molecule. Representations of protein and ATP ligand were prepared using Insight II (27). The partial charges were assigned using the Consistent Valence Force Field. Unless otherwise stated, all H_2O molecules were removed. Atomic solvation parameters and fragmental volumes were assigned to the protein using the Addsol program. The grid maps were calculated using Autogrid and were centered on the putative ligand-binding site (NSP2 cleft). The volume chosen for the grid maps was 81 $\times$ 81 $\times$ 81 points with a grid-point spacing of 0.375 Å. Autotors was used to define the rotatable bonds in the ATP. For the docking simulation of ATP the bonds between Pβ–O3B and Pγ–O3B were restrained, emulating the conformation in which ATP is bound to the Mg^{2+} ion. The Lamarckian Genetic Algorithm was used for all docking calculations.

RESULTS

Selection of Residues in NSP2 for Mutagenesis—The 25-Å-deep cleft between the C- and N-terminal domains of NSP2 encoded by rotavirus SA11 is the proposed site of NTP hydrolysis (Ref. 21 and Fig. 1, *A* and *B*). Within this region, His^{221} was suggested as the first histidine of a HIT-like catalytic triad based on structural superposition with a similar residue (His^{110}) of PKCI, and His^{225} was proposed to be the second histidine of the triad and, possibly, the histidine that carries out the nucleophilic attack (21). Sequence alignment of NSP2 encoded by group A, B, and C rotaviruses shows that residues forming the cleft are highly conserved despite sequence similarity of only ~32% between NSP2 of group A and B rotaviruses and ~55% between NSP2 of group A and C rotaviruses (Fig. 1*D*). The conservation of a cluster of residues in the vicinity of His^{225} suggests the presence of a motif, His^{221}-Gly-(Lys/His)-Xaa-His^{225}-Xaa-Arg-Xaa-Val, within the cleft that may function in NTP binding and hydrolysis. Certainly the presence of conserved basic residues within this motif (His^{221}, Lys/His^{223}, His^{225}, and Arg^{227}) and surrounding it (Lys^{188} and His/Lys^{110}) impart an electropositive surface potential to the cleft that makes it suitable for nucleotide binding. Flanking the motif are highly conserved hydrophobic residues (Leu^{111}, Ile/Val^{157}, Val^{158}, Met/Ile^{167}, Ile/Met^{220}, Val^{229}, and Leu/Val^{234}) that likely participate in maintaining the structural integrity of the cleft. Also located within the cleft are Glu^{153} and Tyr^{171}, residues that based on ordered density peaks noted in the solved structure of NSP2 were proposed to coordinate the binding of Mg^{2+} (21). These putative Mg^{2+}-coordinating residues are conserved among NSP2 encoded by different groups of rotaviruses (Fig. 1*D*).

To identify the NTPase catalytic site, eight residues in the SA11 NSP2 cleft were selected for site-directed mutagenesis based on the x-ray structure of the protein (21), surface exposure (Fig. 1*C*), and the conservation of the residues among group A, B, and C rotaviruses (Fig. 1*D*). These residues, His^{110}, Glu^{153}, Tyr^{171}, Lys^{188}, His^{221}, Lys^{223}, His^{225}, and Arg^{227}, were subsequently mutated to alanine. NSP2 proteins containing a mutation are indicated in italics, *e.g. H110A*. The expression and purification of the NSP2 mutants were carried out following procedures previously established for *wtNSP2* (6). To ensure that the quaternary structure, and hence the multimeric state, of the mutant proteins were comparable to that of *wtNSP2*, the mutant proteins along with protein size markers were subjected to rate zonal centrifugation (6). The sedimentation properties of the NSP2 mutants were indistinguishable from *wtNSP2*, which migrates in a 5–20% sucrose gradient as an ~10 S species (data not shown).

Glu^{153}, Tyr^{171}, Lys^{188}, His^{221}, His^{225}, and Arg^{227} Are Essential for NTPase Activity—NSP2 possesses a Mg^{2+}-dependent NTPase activity that hydrolyzes the β– γ phosphodiester bond of any of the four NTPs with similar efficiency (6). To compare their NTPase activities, wt and mt forms of NSP2 were incubated for 1 h at 37 °C with [α-^{32}P]ATP and $MgCl_2$. The products of the hydrolysis reactions were resolved by TLC and identified by autoradiography (Fig. 2*A*). The average specific NTPase activity of each mutant was determined and then normalized to that of *wtNSP2*. As shown in Fig. 2*B*, most of the NSP2 mutants were affected in their NTPase activity. Based on their NTPase activities, the mutants could be broadly grouped as severely affected (retaining ≤10% of activity), *viz. E153A*, *Y171A*, *K188A*, *H221A*, *H225A*, and *R227A*; moderately affected (retaining ~25% activity), *viz. K223A*; and minimally affected (retaining ~65% activity), *viz. H110A*. Thus, the near complete loss of NTPase activity resulted from mutation of any of the following residues: His^{221} and His^{225}, the first two histidines of the proposed catalytic triad; Lys^{188} and Arg^{227}, conserved basic residues in the cleft; and Glu^{153} and Tyr^{171}, the putative Mg^{2+}-coordinating residues (Fig. 2*B*). Hence these residues have critical roles in the efficient hydrolysis of NTP by NSP2.

Mutation of His^{110} and Lys^{223} yielded proteins that retained ~65 and 25%, respectively, of the NTPase activity of *wtNSP2*, suggesting that these residues may not be directly involved in hydrolysis. Unlike Glu^{153}, Tyr^{171}, Lys^{188}, His^{221}, His^{225}, and Arg^{227} that are strictly conserved in group A, B, and C rotaviruses, His^{110} and Lys^{223} are conserved in groups A and C but not in group B where residue 110 is a lysine and residue 223 is a histidine (Fig. 1*D*). However, the fact that His^{110} and Lys^{223} in group A and C rotaviruses are replaced with similarly basic amino acids in group B viruses suggests that the charges contributed by residues 110 and 223 are conserved and therefore have an important role in optimal NTPase activity.

Modeling of ATP Docking in NSP2—To gain further insight into the interaction of NTP with NSP2, multiple ATP docking simulations were performed with the Autodock 3.02 program. Of the 10 most favored energetic positions (lowest energy), eight predicted ATP binding in one orientation within the cleft, while two predicted ATP binding in the opposite orientation (Fig. 3, *A* and *B*). The two possible nucleotide orientations differed nearly 180° in base and sugar position but displayed a phosphate backbone overlap (Fig. 3*A*). In each of these positions, the ATP is docked in a defined area deep within the cleft and in close proximity to the side chains of Lys^{188}, His^{225}, and Arg^{227} (data not shown). This finding is consistent with the predictions from the crystallographic data (21) and with the results of the NTPase assays that show that mutation of Lys^{188}, His^{225}, or Arg^{227} yields forms of NSP2 that are defective in hydrolysis activity (Fig. 2*B*).

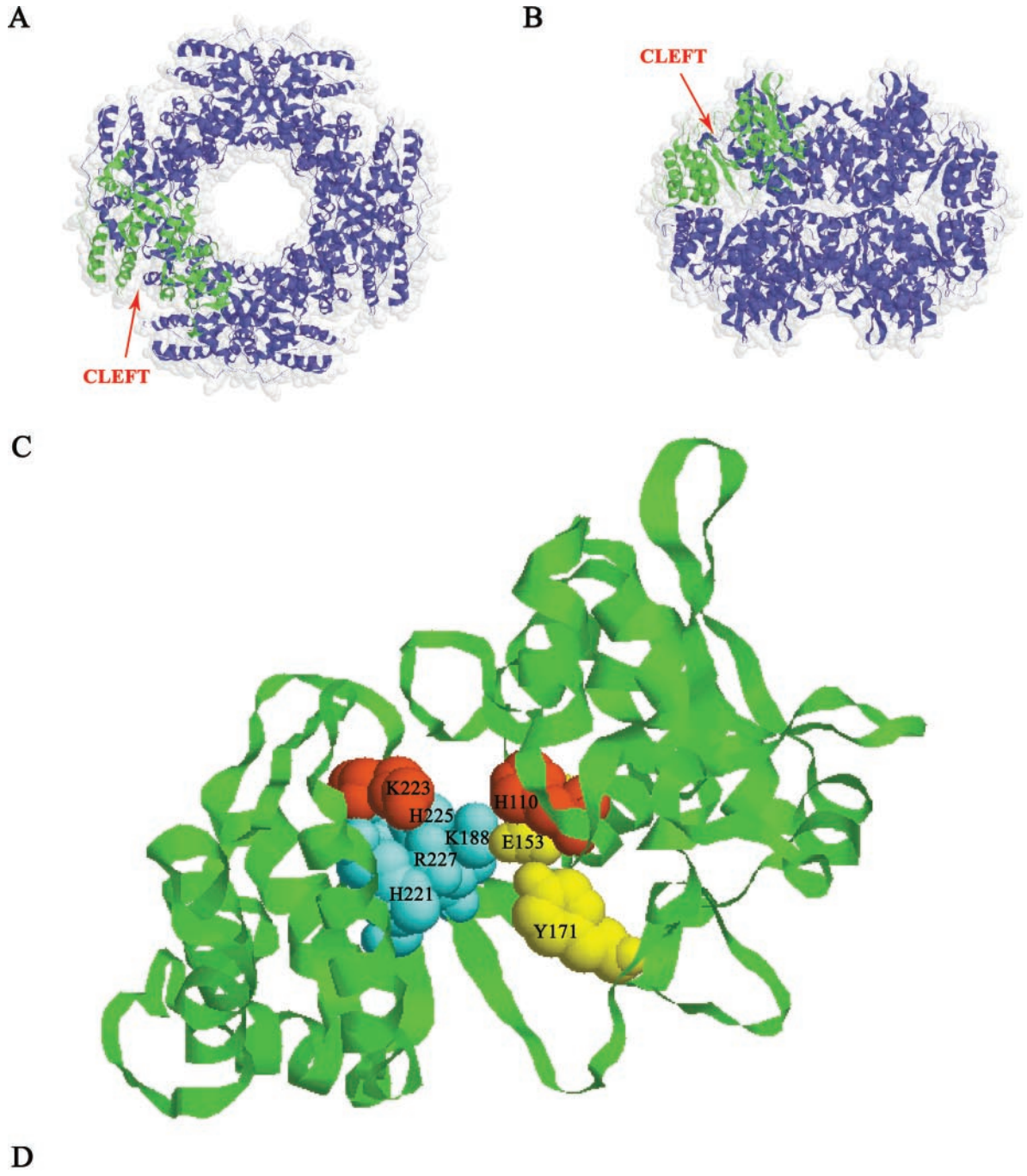

FIG. 1. **Putative site of NTP hydrolysis in the cleft of NSP2.** *A* and *B*, ribbon representation of the NSP2 octamer superimposed on a space-filling model. The 25-Å-deep cleft between the C- and N-terminal domains of one NSP2 monomer (*green*) oriented along 4-fold (*A*) and 2-fold (*B*) axes is indicated. *C*, a close-up view of the NSP2 monomer (strain SA11) highlighting residues predicted to be involved in NTP binding and/or hydrolysis (*red* or *blue*) and Mg^{2+} coordination (*yellow*). *D*, conserved residues in the region of the cleft containing the proposed site for NTP hydrolysis. The GenBank™ accession numbers of the NSP2 proteins are 1L9VA (*SA11 4F*), Q03245 (*WA*), P09366 (*Osu*), BAA84967 (*KU*), P03538 (*UK*), Q03244 (*TY-1*), BAA24142 (*PO-13*), S25545 (*Bovine*), CAB52753 (Bristol (*Brist*)), AAF72868 (*CAL1*), U03558 (*IDIR*), and AAA47328 (*ADRV*). The *numbers at the ends* of the alignment correspond to positions in the primary sequence, while the *numbers in parentheses* represent gap lengths. Conserved residues are *shaded*. Group A, B, and C rotaviruses are indicated at the *left end* of the alignment.

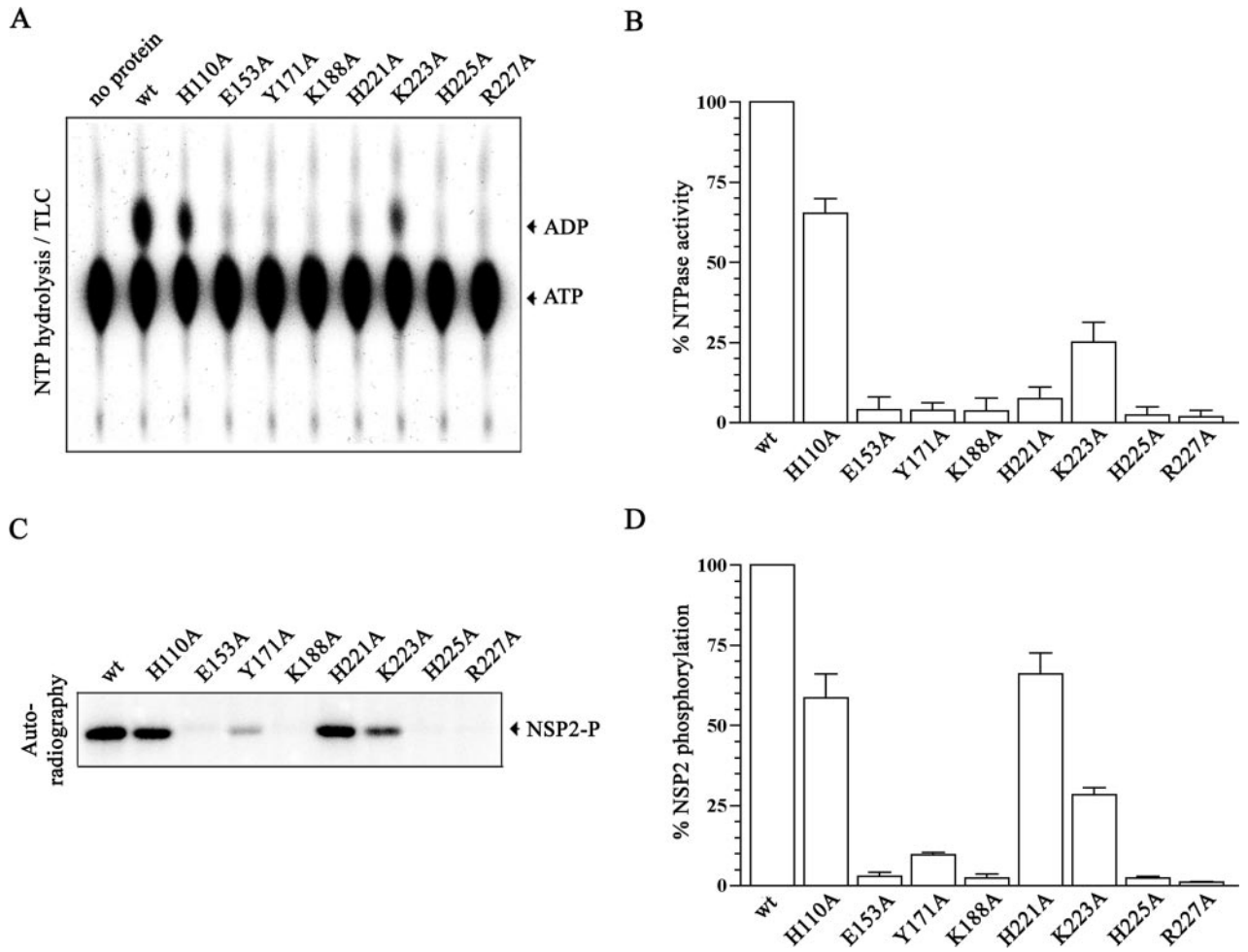

FIG. 2. **NTPase activity and autophosphorylation of NSP2 mutants.** *A*, ^{32}P-labeled ADP generated in reaction mixtures containing no protein, or 28 pmol of wt or mt protein, and 10 μCi of [α-^{32} P]ATP was detected by TLC and autoradiography. *B*, same as *A* except for each protein, five separate but parallel assays were performed differing only in amount of wt or mt NSP2 included (14, 28, 56, 84, or 112 pmol). ^{32}P-Labeled ADP in reaction mixtures was resolved by TLC, quantified with a PhosphorImager, and used to calculate relative specific NTPase activity. Values representing the averages of two independent sets of experiments were reported as a percentage of the *wtNSP2* NTPase activity. *C*, reaction mixtures containing 28 pmol of wt or mt NSP2 and 10 μCi of [γ-^{32}P]ATP were analyzed by SDS-PAGE, and the gel was stained with Coomassie Blue. ^{32}P-Labeled NSP2 was detected by autoradiography. *D*, values determined for phosphorylation of wt and mt NSP2 from three independent experiments were averaged and normalized to *wtNSP2*. *Error bars* represent the S.E. *NSP2-P*, phosphorylated NSP2.

NTP Hydrolysis and NSP2 Autophosphorylation—The NTPase activity of NSP2 results in the autophosphorylation of the protein via covalent linkage of the liberated γ-phosphate (6). To understand the relationship between the NTPase activity of NSP2 and the autophosphorylation of the protein, wt and mt forms of NSP2 were incubated with [γ-^{32}P]ATP under conditions similar to those used in NTPase assays. Radiolabeled NSP2 in the reaction mixtures was detected by SDS-PAGE and autoradiography (Fig. 2*C*) and quantified with a PhosphorImager (Fig. 2*D*). As previously reported (6), the analysis showed that *wtNSP2* undergoes autophosphorylation as a consequence of [γ-^{32}P]ATP hydrolysis.

Little or no autophosphorylation occurred in assays containing *E153A*, *Y171A*, *K188A*, *H225A*, and *R227A*, a finding that correlates well with the observation that these mutants possessed levels of NTPase activity that were ≤10% of *wtNSP2* (Fig. 2*B*). Similarly the levels of *H110A* and *K223A* autophosphorylation were 60 and 30% of *wtNSP2*, respectively, and thus proportional to the levels of NTPase activity associated with these mutants (65 and 25% of *wtNSP2*, respectively). Therefore, analysis of these seven mutants indicated that a strong correlation exists between the extent of autophosphorylation and NTPase activity. In contrast, these activities were uncoupled in the case of *H221A* as this protein, despite being severely affected in its ability to hydrolyze NTPs (<10% NTPase activity) (Fig. 2*B*), retained levels of autophosphorylation that were ≥50% that of *wtNSP2*.

Kinetics of NTP Hydrolysis and Autophosphorylation—The kinetics of NTP hydrolysis by *wtNSP2*, *H221A*, and other mutants of NSP2, *H110A* and *K223A*, possessing at least some NTPase activity were examined by a Michaelis-Menten plot of ATP concentration *versus* rate of ATP hydrolysis (Fig. 4*A*). Estimation of the standard kinetic parameters from the plot showed that the K_m values for *wtNSP2*, *H110A*, *H221A*, and *K223A* were similar, varying by <2-fold (Table I). In contrast, the V_{max} value for *H221A* was ~18-fold less than that of *wtNSP2*, while those for *H110A* and *K223A* were ~2- and 4-fold less than *wtNSP2*, respectively (Table I). These data indicate that the H221A mutation causes a reduction in the rate of NTP hydrolysis by NSP2 without significantly affecting substrate (NTP) binding.

To obtain further insight into the mechanism by which His^{221} achieved intermediate levels of phosphorylation although it was severely deficient in NTPase activity (Fig. 2, *B* and *D*), its rate of NTP hydrolysis and autophosphorylation were compared with those of *wtNS2P*, *H110A*, and *K223A* as a function of time. The assays were performed by collecting aliquots during a 1-h incubation period from reaction mixtures

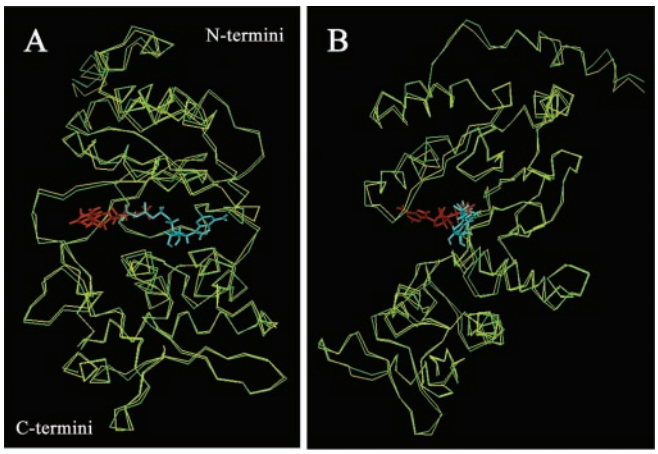

FIG. 3. **Modeling of ATP docking in the NSP2 cleft.** Results from molecular docking of ATP in the cleft of the NSP2 monomer as predicted by Autodock 3.02. *A*, two independent models were superimposed to show the two possible orientations of the ATP molecule (colored *red* or *blue*) in the cleft of the monomer. *B*, view of the molecule as shown in *A* with a 90° rotation along the *y* axis.

containing [γ-^{32}P]ATP and then analyzing the aliquots for NTP hydrolysis by TLC and for autophosphorylation by SDS-PAGE. The results showed that autophosphorylation of *wtNSP2* reached a maximum at 30 min of incubation, although the level of NTP hydrolysis increased during the entire incubation period (60 min) (Fig. 4, *B* and *C*). In contrast, the extent of autophosphorylation for *H221A* increased gradually over the incubation period and reached levels that were maximal at a time later than that seen for either *wtNSP2*, *H110A*, or *K223A*. Notably the extent of maximal phosphorylation for *H221A* (50–60 min of incubation) reached 50% of that of *wtNSP2* (30 min of incubation) despite the fact that at any given time during the incubation period the level of NTP hydrolysis by the *H221A* protein was <10% of that of *wtNSP2*. The analysis also revealed that although the NTPase activities of *H110A* and *K223A* were substantially higher than that of *H221A*, the extent of phosphorylation reached by *H110A* or *K223A* was the same or less than that reached by *H221A*. Collectively these findings suggest that the rate of NTP hydrolysis is not the only determinant of NSP2 autophosphorylation.

Stability of the Phosphorylated Intermediate of NSP2—Another factor that may influence the level of NSP2 phosphorylation is the stability of its phosphorylated amino acid, specifically the susceptibility of its phosphoamino acid bond to hydrolysis. Since phosphoramidate (P–N) and phosphoester (P–O) bonds vary in their susceptibility to hydrolysis under acid and alkaline conditions (28), the nature of the phosphoamino acid linkage in NSP2, formed during NTP hydrolysis, was analyzed as a function of pH. In the assay, NSP2 was incubated with [γ-^{32}P]ATP for 1 h at 37 °C, and as a control, CKII, a protein whose β-subunit is phosphorylated at serine residues (29, 30), was incubated in a parallel reaction for 1 h at 30 °C. The protein products of the reaction were resolved by SDS-PAGE, transferred to a polyvinylidene difluoride membrane, and subsequently treated for 2 h at 65 °C with either 1 M KOH or 6 M HCl. The radiolabeled proteins after the acid/alkaline treatment were identified by autoradiography. As shown in Fig. 5*A*, the phosphoamino acid bond formed in NSP2, unlike that formed in CKII-β subunit, is stable under alkaline conditions and unstable under acid conditions. Since P–O linkages are characteristically susceptible to alkaline conditions while P–N linkages are not (28, 31), the result suggests that hydrolysis of NSP2 proceeds via a covalent phosphoramidate (P–N) linkage. Given its similarity to HIT proteins, NSP2 may

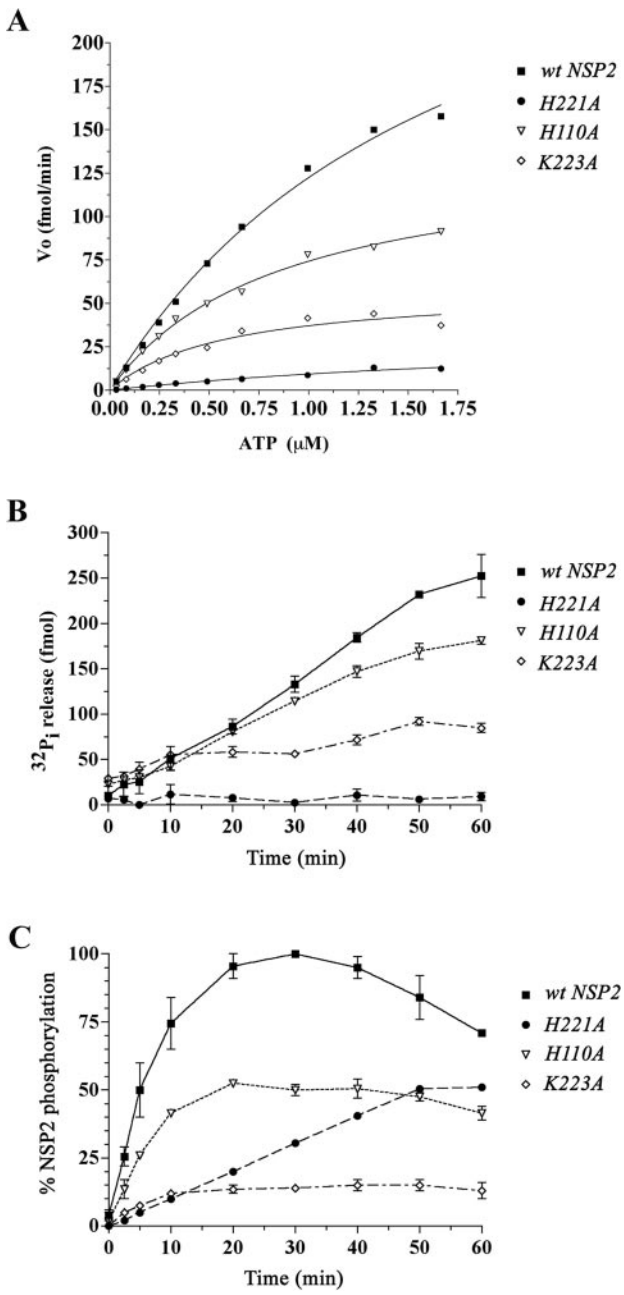

FIG. 4. **Relationship between NSP2 NTP hydrolysis and autophosphorylation.** *A*, kinetics of ATP hydrolysis. Reaction mixtures containing 50 mM Tris-HCl (pH 7.5), 5 mM $MgCl_2$, 9.8 pmol of either wt or mt NSP2, and increasing concentrations of [γ-^{32}P]ATP in a total volume of 10 μl were incubated at 37 °C for 1 h. ATP hydrolysis was monitored by TLC. The rate of $^{32}P_i$ release (V_o) in fmol/min was plotted as a function of ATP concentration. *B*, reaction mixtures containing wt or mt NSP2 and 0.1 μM [γ-^{32}P]ATP were incubated at 37 °C for the indicated periods of time. ATP hydrolysis was monitored by analyzing one-half of each reaction mixture for $^{32}P_i$ release by TLC. *C*, NSP2 phosphorylation was monitored by analyzing the other half by SDS-PAGE. Levels of $^{32}P_i$ release and ^{32}P-labeled NSP2 were determined, and for the latter the levels were normalized with the highest value obtained for *wtNSP2* set at 100%.

be similarly phosphorylated during NTP hydrolysis to produce a phosphohistidine reaction intermediate (22, 32).

The rate of release of the phosphate group from histidine, the result of a second nucleophilic attack, is significantly influenced by neighboring amino acids (31). It is possible that mutations introduced in NSP2 near the active site for NTP hydrolysis may affect this second step in hydrolysis and thereby affect the stability of phosphorylated intermediate. To assess

TABLE I
Kinetic parameters of the NTPase activity of wt and mt NSP2

Protein	V_{max} [a,b]	K_m [a]
	fmol/min	*μM*
wtNSP2	18	0.650
H110A	9	0.425
H221A	1	0.635
K223A	4	0.375

[a] The values for V_{max} and K_m were determined from hyperbolic fits to the Michaelis-Menten equation by nonlinear regression using Prism 3.0 (GraphPad Software).
[b] V_{max} was reported as the turnover number in fmol of product (P_i) formed/min/pmol of enzyme.

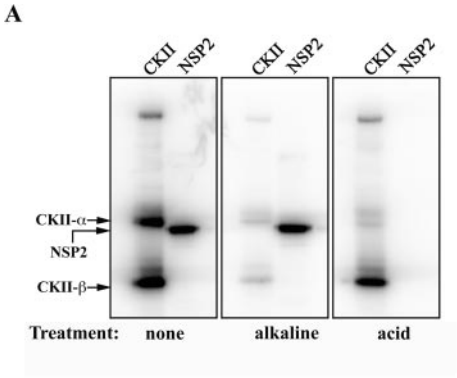

FIG. 5. **Stability of the phosphoamino acid of *wtNSP2* and *H221A*.** *A*, to assess the hydrolytic stability of NSP2 under acid/alkaline conditions, reaction mixtures containing 28 pmol of NSP2 or 500 units of CKII and 10 μCi of [γ-^{32}P]ATP (3,000 Ci/mmol) in a final volume of 20 μl were incubated for 1 h at 37 °C and 30 min at 30 °C, respectively. Phosphorylated proteins were separated by 12% SDS-PAGE and transferred to polyvinylidene difluoride membrane. Membranes were air-dried and autoradiographed after incubation under acid or alkaline conditions for 2 h at 65 °C. Although both CKII α-and β subunits are phosphorylated, only the β-subunit served as a control for O–phosphate linkage (29, 30) since the nature of the phosphoamino linkage in CKII-α is not known. *B*, reaction mixtures containing 28 pmol of *wtNSP2* or *H221A* and 10 μCi of [γ-^{32}P]ATP were incubated at 37 °C for 2 h. After 1 h of incubation, some reaction mixtures were adjusted to 50 mM EDTA. Samples recovered during the assay were analyzed by SDS-PAGE, and levels of ^{32}P-labeled NSP2 were determined with a PhosphorImager. The highest values of *wtNSP2* phosphorylation were defined as 100%.

whether the stability of the phosphoamino acid in *wtNSP2* differed from that of *H221A*, reaction mixtures were prepared that contained either the wt or mt protein, [γ-^{32}P]ATP, and $MgCl_2$. After 1 h of incubation, further NTP hydrolysis was blocked in some reaction mixtures by the addition of EDTA to chelate Mg^{2+}, a cofactor required for the NTPase activity of NSP2. After incubation of reaction mixtures for an additional

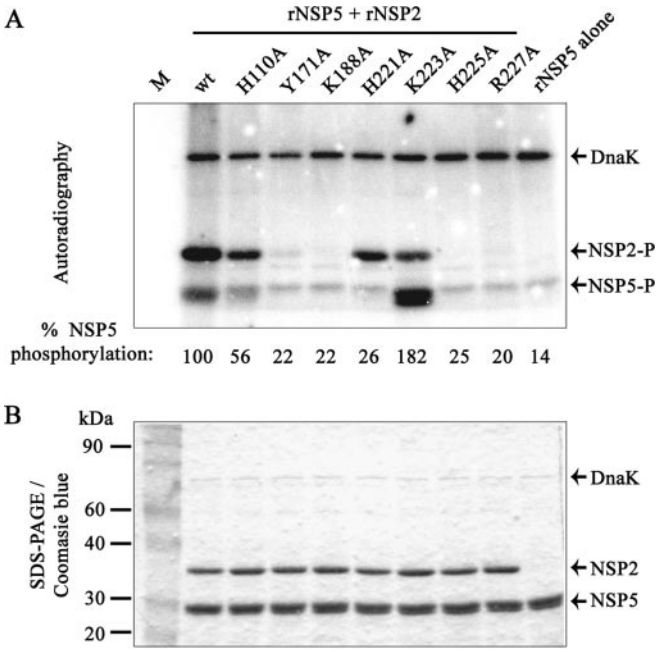

FIG. 6. **Effect of NSP2 NTPase activity on NSP5 phosphorylation *in vitro*.** NSP5 (70 pmol) was incubated alone or with wt or mt forms of NSP2 (28 pmol) and [γ-^{32}P]ATP. After incubation for 2 h at 37 °C, proteins in the mixtures were resolved by 12% SDS-PAGE and stained with Coomassie Blue (*B*). Radiolabeled proteins were detected by autoradiography (*A*) and quantified with a PhosphorImager. *M*, molecular weight markers; *NSP2-P*, phosphorylated NSP2; *NSP5-P*, phosphorylated NSP5.

1 h, aliquots recovered from the mixtures during the course of the assay were analyzed for levels of phosphorylated NSP2. The results showed that inhibition of hydrolysis with EDTA was followed by an increasing loss over time in the amount of phosphorylated *wtNSP2* and *H221A* in reaction mixtures (Fig. 5*B*). However, the rate of loss was significantly greater for the wt protein than for the mt protein, and the extent of phosphorylation of the wt protein reached a lower level of phosphorylation than was observed for *H221A*. These data suggest that as a consequence of introducing the H221A mutation into NSP2, the phosphoamino acid of *H221A* becomes more stable than that of the wt protein. This characteristic provides a possible explanation as to how His^{221} can reach a relatively high degree of phosphorylation although containing a very low level of associated NTPase activity.

NTP Hydrolysis by NSP2 and the Phosphorylation of NSP5 in Vitro—NSP2 causes a marked increase in the phosphorylation of NSP5 both *in vitro* and *in vivo* (16, 17). NSP2 may mediate NSP5 phosphorylation either by generating inorganic phosphates through its NTPase activity that are transferred to NSP5 or by interacting with NSP5 to activate a dormant autokinase activity. To test for a relationship between the NTPase activity of NSP2 and the phosphorylation of NSP5, wt and mt forms of NSP2 were incubated with purified recombinant NSP5 in the presence of [γ-^{32}P]ATP and $MgCl_2$. The proteins were then analyzed by SDS-PAGE and autoradiography (Fig. 6, *A* and *B*). As reported before, small amounts of the bacterial protein DnaK co-purified with NSP5 and became labeled in phosphorylation assays due to its affinity for ATP (17).

When incubated alone in reaction mixtures, NSP5 underwent a low level of phosphorylation due to its low level of associated autokinase activity (14, 15, 33). When incubated with *wtNSP2*, the extent of NSP5 phosphorylation increased 5–10-fold (Fig. 6*A*). In contrast, incubation with any of the five mutant proteins possessing little or no NTPase activity

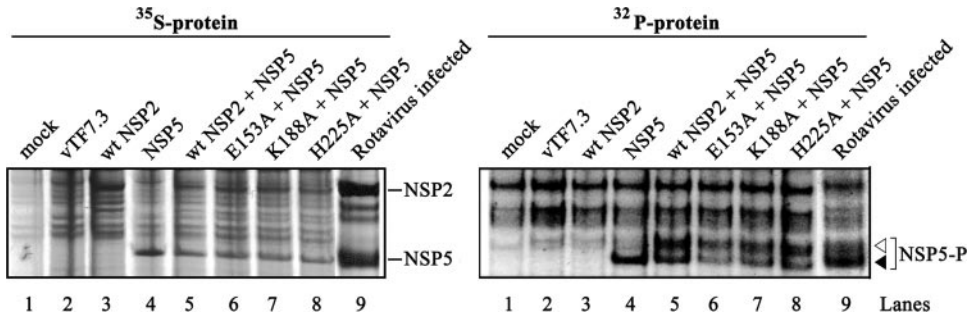

FIG. 7. **Effect of NSP2 NTPase activity on NSP5 hyperphosphorylation *in vivo*.** MA104 cells, infected with vaccinia virus vTF7.3, were programmed to express wt or mt forms of NSP2 and/or NSP5 by transfection with appropriate T7 transcription vectors. As a control, some cells were infected with rotavirus SA11. Cells were maintained in [^{35}S]methionine or [^{32}P]orthophosphate, and NSP2 and NSP5 in cell lysates were analyzed by SDS-PAGE and autoradiography. The phosphorylated 28-kDa (*closed arrow*) and hyperphosphorylated (*open arrow*) forms of NSP5 are indicated. *NSP5-P*, phosphorylated NSP5.

(*Y17A1*, *K188A*, *H221A*, *H225A*, and *R227A*) (Fig. 2*B*) had little (<2-fold) effect on NSP5 phosphorylation. These results indicated that the phosphorylation of NSP5 *in vitro* requires the hydrolysis of NTPs by NSP2. Indeed this is consistent with the observation that NSP5 phosphorylation occurred only in those reaction mixtures in which forms of NSP2 were present that have associated NTPase activity (*H110A* and *K223A*). However, the extent of NSP5 phosphorylation was found not to be directly coupled to the extent of NTP hydrolysis. For example, although the level of NTPase activity for *K223A* was much lower than that of *H110A* (Fig. 2*B*), *K223A* was associated with a much greater level of NSP5 phosphorylation than was *H110A*.

Notably we also observed a lack of a direct connection between NSP2 autophosphorylation and NSP5 phosphorylation. For instance, while the extent of *H221A* phosphorylation was greater than that of *K223A*, *H221A* did not stimulate the phosphorylation of NSP5, while *K223A* stimulated a high degree of NSP5 phosphorylation (Fig. 6*A*). Thus, NSP5 phosphorylation *in vitro* probably does not occur via the direct transfer of a phosphate group from a phosphoamino acid of NSP2 to NSP5.

NTP Hydrolysis by NSP2 and the Phosphorylation of NSP5 in Vivo—Several phosphorylated isoforms of NSP5 of 28 and 32–34 kDa, similar to those seen in rotavirus-infected cells, are observed when NSP2 and NSP5 are co-expressed in uninfected cells (16). To test whether NSP5 phosphorylation *in vivo* is dependent on the NTPase activity of NSP2 as seen *in vitro* (Fig. 6), *wtNSP2* and three NSP2 mutants with little or no NTPase activity (*E153A*, *K188A*, and *H225A*) were transiently expressed with NSP5 in MA104 cells. Proteins made in the cells were labeled with [^{35}S]methionine or [^{32}P]orthophosphate and analyzed by SDS-PAGE and autoradiography (Fig. 7). The results showed that, when NSP5 was expressed alone, only the 28-kDa phosphorylated form (*closed arrow*) of the protein was produced (*lane 4*). In contrast, when *wtNSP2* or *E153A*, *K188A*, or *H225A* was expressed with NSP5, hyperphosphorylated forms (*open arrow*) were readily formed in the cells (*lanes 5–8*). Furthermore the quantity of the ^{32}P-labeled hyperphosphorylated form relative to the 28-kDa phosphorylated form was similar in cells that expressed wt or any of the mt forms of NSP2. Thus, NSP2 mutants lacking NTPase activity were able to induce the hyperphosphorylation of NSP5 *in vivo* just as effectively as *wtNSP2*. This is in contrast to the results of *in vitro* assays, which showed that NSP2 mutants lacking NTPase activity were not able to induce NSP5 phosphorylation. Thus, the mechanism by which NSP2 mediates NSP5 phosphorylation *in vitro* may differ fundamentally from the mechanism operating *in vivo*. This is further illustrated by the observation that hyperphosphorylation *in vivo* produces isoforms of NSP5 of which some migrate electrophoretically more slowly than the initial 28-kDa form of the protein. In contrast, NSP2-mediated phosphorylation of NSP5 *in vitro* does not generate similar slow migrating isoforms of the protein.

Importance of NTPase Activity on the Formation of NSP2-NSP5 Inclusions—Transient expression of NSP2 and NSP5 in uninfected MA104 cells not only leads to the hyperphosphorylation of NSP5 but also to the formation of viroplasm-like structures that are reminiscent of viroplasms that form in rotavirus-infected cells (Fig. 8) (13). Expressed separately, NSP2 and NSP5 distribute much more evenly throughout the cell and do not form large punctate inclusions that are observed when NSP2 and NSP5 are expressed together (Fig. 8). To determine whether the NTPase activity of NSP2 is required for the formation of viroplasm-like structures, two NSP2 mutants (*E153A* and *K188A*) defective in NTPase activity were co-expressed in MA104 cells with NSP5. Immunofluorescence analysis showed that the mutant proteins co-localized with NSP5 in the cells to form viroplasm-like structures. This indicates that the NTPase activity of NSP2 is not required for the protein to participate in the assembly of inclusions. Instead it seems more likely that the NTPase activity of the protein is more likely associated with a process occurring postassembly of the viroplasm.

DISCUSSION

This study identifies a site for NTP binding and hydrolysis deep in the 25-Å-deep cleft created between the C- and N-terminal domains of the NSP2 monomer. The location of this site was predicted earlier, a consequence of the observation that NSP2 has partial structural homology with a member of the HIT family of nucleotidyl hydrolases (21). This structural homology, combined with our results, shows that histidines play a critical role in NTP binding and hydrolysis as is characteristic of HIT proteins.

The crystal structure of NSP2 revealed that its C-terminal ~80-amino acid region folds into a distinct domain made of twisted antiparallel β-sheets surrounded by a central α-helix, which overall displays striking similarity to the C terminus of PKCI, a representative member of one subfamily of HIT proteins (21, 34). Within this region of NSP2, His^{225} was proposed to serve as the catalytic residue for NTP hydrolysis since its position was homologous to His^{112} (within a distance of 1 Å), the second histidine and catalytic residue of the histidine triad of PKCI (21, 22). Consistent with the suggestion that His^{225} is the catalytic residue, its mutation to alanine resulted in a dramatic loss of NTPase activity. In addition, mutation of conserved residues located in the cleft near His^{225}, *i.e.* Lys^{188}, His^{221}, and Arg^{227}, also severely affected the NTPase activity. Thus, despite the lack of sequence similarity between NSP2 and PKCI and the absence of a classic HIT motif (HØHØHØØ)

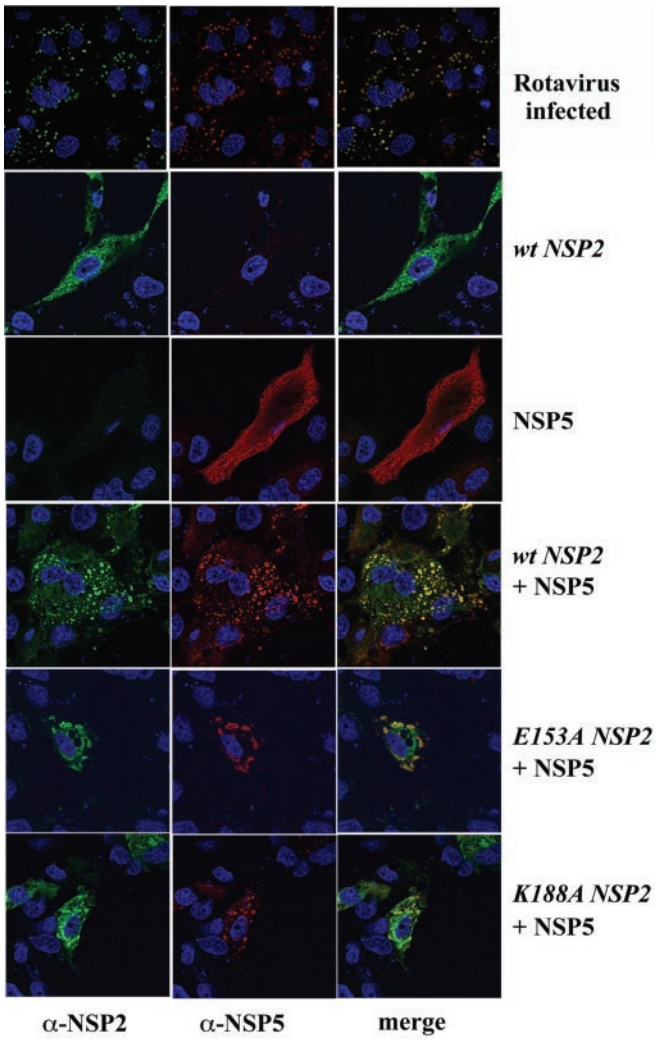

FIG. 8. **Importance of NSP2 NTPase activity on the formation of viroplasm-like structures.** MA104 cells were infected with rotavirus SA11 or vaccinia virus vTF7.3. The vTF7.3 cells were transfected with T7 transcription vectors encoding wt or mt forms of NSP2 and/or NSP5. The distribution of NSP2 and NSP5 in the cells was assessed by incubation with NSP2-specific guinea pig polyclonal and NSP5-specific mouse monoclonal antisera followed by goat anti-guinea pig Alexa488 (*green*) and anti-mouse Alexa594 (*red*) secondary antibodies, respectively. Nuclei were visualized by staining with 4,6-diamidino-2-phenylindole. Immunostained cells were analyzed by confocal laser scanning microscopy. Co-localization of NSP2 and NSP5 is represented by *yellow* in the merged images.

in NSP2, the proteins retain a similar site for NTP binding and/or hydrolysis.

Additional support for the idea that His^{225} and neighboring residues of the cleft form an NTP-binding site was provided by computer-based ATP docking simulations that showed that the most energy-favorable interactions occurred between ATP and residues that are in the vicinity of His^{225}, notably Lys^{188} and Arg^{227}. The analysis also indicated that the characteristics of the cleft, especially its highly electropositive nature, may impact on optimal NTP binding. The docking predictions also revealed that NTP binding in the cleft was guided by the phosphate backbone and not the nucleoside moiety of the substrate providing an explanation for the lack of specificity observed for the NTPase activity of NSP2. Indeed the lack of recognition for the nucleoside moiety raises the possibility that other molecules containing polyphosphates, *e.g.* the 5′-γ-phosphate of RNA, may serve as substrates for the hydrolysis activity of NSP2.

Despite the similarities of their structures and active sites, NSP2 differs from PKCI and other known HIT proteins in substrate specificity, Mg^{2+} dependence for hydrolysis, and oligomeric status (21, 22, 34). Notably, unlike NSP2 octamers that hydrolyze NTPs via a Mg^{2+}-dependent mechanism to liberate γ-phosphates, most HIT proteins are dimers that cleave dinucleotide polyphosphates (*e.g.* ApppA) via a cation-independent mechanism to liberate monophosphate nucleotides (22, 32, 34). These differences raise the possibility that NSP2 and the HIT proteins differ fundamentally in the mechanism by which they hydrolyze nucleotide substrates although displaying a high degree of similarity in the make-up of their active sites. In our analysis, we noted that mutation of Glu^{153} and Tyr^{171}, the two residues of the cleft proposed to coordinate the binding of Mg^{2+}, resulted in a loss of NTPase activity. This loss of activity is consistent with the observed necessity for the cation in NTP hydrolysis by NSP2. However, we have also found using photoreactable analogs that NSP2 efficiently binds NTPs even in the absence of Mg^{2+} (data not shown). Thus, neither NSP2 nor the HIT proteins require Mg^{2+} for the docking of their nucleotide substrates. Instead it is apparently in the hydrolysis of their substrates that NSP2 and the HIT proteins differ in their requirements for a cation. Since Mg^{2+} can have an effect on the conformation of an NTP (22, 35), the presence of the cation may be important for positioning an NTP in the cleft in such a way as to allow for hydrolysis.

NTP hydrolysis by NSP2 is accompanied by the autophosphorylation of the protein (6). Although such phosphorylation requires NTP hydrolysis, the net accumulation of the phosphorylated species of NSP2 is disproportionately low compared with the amount of product that is generated (NDP + P_i) (Fig. 2). The phosphorylated species is not stable, undergoing rapid dephosphorylation upon inhibition of the hydrolysis activity of the protein (Fig. 5). These characteristics taken together suggest that cleavage of the γ-phosphate is followed by the formation of a transient intermediate where the phosphate becomes covalently bound to NSP2 via a phosphoramidate linkage. The rate of dephosphorylation is slower than the rate of phosphorylation, which accounts for the detection of the phosphorylated species of NSP2 in NTPase assays. The release of the bound phosphate from the protein (dephosphorylation) must require a second nucleophilic attack. For most HIT proteins, the third histidine of the histidine triad activates water and thereby drives the second attack (22, 32). Although NSP2 lacks a strict histidine triad, a water molecule in close proximity to the NTP-binding site could function in a second nucleophilic attack. Our studies indicate that His^{221} is also involved in the second attack since phosphorylated *H221A* undergoes dephosphorylation at a rate that is considerably slower than phosphorylated *wtNSP2*. The inability of *H221A* to undergo efficient dephosphorylation may affect the ability of the protein to be recycled and thereby support additional rounds of NTP hydrolysis. Thus, the slow rate of dephosphorylation may be responsible for the remarkably low level of NTPase activity that is associated with *H221A*.

NSP2 stimulates the phosphorylation of NSP5 *in vitro* and the hyperphosphorylation of NSP5 *in vivo* (Figs. 6 and 7). Our studies show that the NTPase activity of NSP2 is necessary for the phosphorylation of NSP5 but only outside the context of the cell, i.e. pertaining to purified recombinant proteins. When cellular proteins are present that are known to affect the net phosphorylation of NSP5 (*e.g.* kinases and phosphatases) (36), NSP5 hyperphosphorylation requires the presence of NSP2 but not its NTPase activity (Fig. 7). This observation suggests that during virus replication, hyperphosphorylation is not the consequence of a phosphotransfer reaction between NSP2 and

NSP5 (17). Instead it seems more likely that hyperphosphorylation derives from an autokinase activity of NSP5 and that the activation of the autokinase activity requires the interaction of NSP5 with NSP2 and cellular factors (*e.g.* kinases). The purpose of NSP5 hyperphosphorylation is not known, but this modification occurs even in cells that are not rotavirus-infected and thus is not dependent on virus replication.

NSP2 and NSP5 play a critical role in the viral life cycle by triggering the formation of cytoplasmic inclusions that localize virus genome packaging and replication and early stages of virion morphogenesis to defined boundaries in the infected cell (10, 12). Although the role of the NTPase activity of NSP2 in the viral life cycle is not known, our analyses allow us to exclude the possibility that the activity has a role in the assembly of inclusions. It is interesting to note that the inclusion-forming protein NS2 of bluetongue virus, another member of the Reoviridae, also has strong nucleotidyl phosphatase activity and is multimeric (37, 38). Despite similarities in the structure and function of NS2 and NSP2, these proteins display a near complete lack of sequence identity. Notably NS2 lacks a sequence that is overtly similar to that which represents the NTP-binding and hydrolysis sites of either HIT proteins or NSP2. Whether a HIT-like fold exists in NS2 awaits solution of its x-ray structure. As yet, rotavirus NSP2 is the only known viral protein with a HIT-like fold and active site that functions in the binding and hydrolysis of NTP. These features signify that NSP2 may represent a new and distinct group of viral nucleotidyl hydrolases.

Acknowledgments—Computer resources were provided in part by the NCI, National Institutes of Health, Frederick Biomedical Supercomputer Center through collaboration between Dr. Raul Cachau and F. D. González-Nilo. We thank Dr. Emilio Cardemil at the University of Santiago of Chile for providing computer facilities. We are grateful to Megan T. Collins and Maria T. Castillo for excellent technical assistance.

REFERENCES

1. Parashar, U. D., Hummelman, E. G., Bresee, J. S., Miller, M. A., and Glass, R. I. (2003) *Emerg. Infect. Dis.* **9,** 565–572
2. Kapikian, A. Z., Hoshino, Y., and Chanock, R. M. (2001) in *Fields Fundamental Virology* (Knipe, D. M., and Howley, P. M., eds) 4th Ed., pp. 1787–1833, Lippincott Williams & Wilkins Press, Philadelphia
3. Ramig, R. F., and Petrie, B. L. (1984) *J. Virol.* **49,** 665–673
4. Chen, D., Gombold, J. L., and Ramig, R. F. (1990) *Virology* **178,** 143–151
5. Kattoura, M. D., Chen, X., and Patton, J. T. (1994) *Virology* **202,** 803–813
6. Taraporewala, Z., Chen, D., and Patton, J. T. (1999) *J. Virol.* **73,** 9934–9943
7. Taraporewala, Z. F., and Patton, J. T. (2001) *J. Virol.* **75,** 4519–4527
8. Schuck, P., Taraporewala, Z., McPhie, P., and Patton, J. T. (2001) *J. Biol. Chem.* **276,** 9679–9687
9. Gonzalez, S. A., and Burrone, O. R. (1991) *Virology* **182,** 8–16
10. Petrie, B. L., Greenberg, H. B., Graham, D. Y., and Estes, M. K. (1984) *Virus Res.* **1,** 133–152
11. Gonzalez, R. A., Torres-Vega, M. A., Lopez, S., and Arias, C. F. (1998) *Arch. Virol.* **143,** 981–996
12. Petrie, B. L., Graham, D. Y., Hanssen, H., and Estes, M. K. (1982) *J. Gen. Virol.* **63,** 457–467
13. Fabbretti, E., Afrikanova, I., Vascotto, F., and Burrone, O. R. (1999) *J. Gen. Virol.* **80,** 333–339
14. Afrikanova, I., Miozzo, M. C., Giambiagi, S., and Burrone, O. (1996) *J. Gen. Virol.* **77,** 2059–2065
15. Poncet, D., Lindenbaum, P., L'Haridon, R., and Cohen, J. (1997) *J. Virol.* **71,** 34–41
16. Afrikanova, I., Fabbretti, E., Miozzo, M. C., and Burrone, O. R. (1998) *J. Gen. Virol.* **79,** 2679–2686
17. Vende, P., Taraporewala, Z. F., and Patton, J. T. (2002) *J. Virol.* **76,** 5291–5299
18. Kattoura, M. D., Clapp, L. L., and Patton, J. T. (1992) *Virology* **191,** 698–708
19. Helmberger-Jones, M., and Patton, J. T. (1986) *Virology* **155,** 655–665
20. Gallegos, C. O., and Patton, J. T. (1989) *Virology* **172,** 616–627
21. Jayaram, H., Taraporewala, Z., Patton, J. T., and Prasad, B. V. (2002) *Nature* **417,** 311–315
22. Lima, C. D., Klein, M. G., and Hendrickson, W. A. (1997) *Science* **278,** 286–290
23. Mitchell, D. B., and Both, G. W. (1988) *Nucleic Acids Res.* **16,** 6244
24. Fuerst, T. R., Niles, E. G., Studier, F. W., and Moss, B. (1986) *Proc. Natl. Acad. Sci. U. S. A.* **83,** 8122–8126
25. Brooks, B. R., Bruccoleri, R. E., Olafson, B. D., States, D. J., Swaminathan, S., and Karplus, M. (1983) *J. Comp. Chem.* **4,** 187–217
26. Morris, G. M., Goodsell, D. S., Halliday, R. S., Huey, R., Hart, W. E., Belew, R. K., and Olson, A. J. (1998) *J. Comp. Chem.* **19,** 1639–1662
27. Accelrys (1997) *Insight II and Delphi User Guide*, Accelrys, San Diego, CA
28. Hildebrandt, E., and Fried, V. A. (1989) *Anal. Biochem.* **177,** 407–412
29. Litchfield, D. W., Lozeman, F. J., Cicirelli, M. F., Harrylock, M., Ericsson, L. H., Piening, C. J., and Krebs, E. G. (1991) *J. Biol. Chem.* **266,** 20380–20389
30. Hinrichs, M. V., Jedlicki, A., Tellez, R., Pongor, S., Gatica, M., Allende, C. C., and Allende, J. E. (1993) *Biochemistry* **32,** 7310–7316
31. Klumpp, S., and Krieglstein, J. (2002) *Eur. J. Biochem.* **269,** 1067–1071
32. Brenner, C. (2002) *Biochemistry* **41,** 9003–9014
33. Blackhall, J., Fuentes, A., Hansen, K., and Magnusson, G. (1997) *J. Virol.* **71,** 138–144
34. Brenner, C., Bieganowski, P., Pace, H. C., and Huebner, K. (1999) *J. Cell. Physiol.* **181,** 179–187
35. McIntosh, D. B., Clausen, J. D., Woolley, D. G., MacLennan, D. H., Vilsen, B., and Andersen, J. P. (2003) *Ann. N. Y. Acad. Sci.* **986,** 101–105
36. Eichwald, C., Vascotto, F., Fabbretti, E., and Burrone, O. R. (2002) *J. Virol.* **76,** 3461–3470
37. Horscroft, N. J., and Roy, P. (2000) *J. Gen. Virol.* **81,** 1961–1965
38. Taraporewala, Z. F., Chen, D., and Patton, J. T. (2001) *Virology* **280,** 221–231